# Molten salt corrosion mechanisms of nitrate based thermal energy storage materials for concentrated solar power plants: A review

**Ángel G. Fernández, Luisa F. Cabeza**

*GREiA Research Group, INSPIRES Research Centre, Universitat de Lleida, Pere de Cabrera s/n, 25001 Lleida, Spain*

**Corresponding author:* lcabeza@diei.udl.cat

## Abstract

Corrosion mechanisms for current heat transfer fluid and storage media used in CSP plants working at temperatures from 300ºC to 600ºC are reviewed in this paper. The studies found in the literature show that these mechanisms are influenced by the impurities present in the salt and the relation between $Mg(NO_3)_2$, moisture, $CO_2$, perchlorates, and sulphates with the corrosion process. Corrosion mechanisms were identified along with a discussion of the corrosion products and their influence on the corrosion layers formed.

Keywords: Molten salt, Corrosion mechanisms, Concentrated solar power, Thermal energy storage

## 1. Introduction

Concentrated solar power (CSP) technology captures and stores the sun energy in the form of heat, using low cost materials with high thermal and chemistry stability for decades [1]. Thus, CSP with thermal energy storage (TES) is an effective solution to the integration challenge, delivering renewable energy while providing important capacity, reliability, and stability to the grid while also enabling increased penetration of variable-generation renewable electricity technologies. Today most advanced CSP systems are towers integrated with two-tank molten-salts TES, delivering thermal energy at 565°C for its integration in conventional steam-Rankine power cycles **[1].** This design lowered the cost of CSP electricity by about 50% over the prior generation of parabolic trough systems **[1];** however, the decrease in cost of CSP technologies did not keep pace with the falling cost of solar photovoltaic (PV) systems, therefore further research is needed [1].

The current state-of-the-art power tower designs use a nitrate molten-salt mixture (60wt.%$NaNO_3$+40wt.%$KNO_3$), and different ternary molten salts were proposed to replace them [2], nevertheless, there are still some issues regarding the corrosion mechanism of this fluids with the container metals that need to be controlled.

The costs attributed to corrosion damage were estimated to be on the order of 3% to 5% of industrialized countries gross national product (GNP) [3]. But it is not clear exactly how much cost to attribute to specific problems.

Corrosion can be prevented by changing the composition of the containment material, altering the environment, or separating the metallic bulk of the containment material from the environment through the presence of protective layers at the metal surface [3]. Some corrosion mitigation approaches are the following:

1. Control of alloy chemistry by increasing the presence of protective elements and decreasing the presence of more active (easy to corrode) elements.
2. Control of molten-salt chemistry by purification processes or the use of inhibitors (redox-control or oxidizer getters).
3. Surface treatments, the use of coatings, and/or surface passivation.

Molten-salts corrosion attack can occur by different mechanisms, but quantitative data for materials selection and performance prediction using commercial nitrate salts are rarely available, and corrosion mechanisms are related with the different anions and cations in the molten salts system.

The present paper analyses the nitrate molten salt corrosion mechanism and the impurity influence in the protective scale formation, depending on the maximum operating temperature for the commercial application at temperatures between 300ºC–600ºC using alkali and alkaline-earth nitrate molten salts.

## 2. Molten-salt corrosion mechanisms using alkali and alkaline-earth nitrate molten salts

In current CSP plants, the corrosion caused by the molten-salts heat transfer fluid (HTF) or storage media on the steel containment materials is one of the most important parameters being evaluated. The molten salts currently used (60wt.% $NaNO_3$ + 40wt.% $KNO_3$) presents a melting point around 223ºC [7], so high temperatures are required to maintain the mixtures liquid so they are able to flow. The corrosion of molten-nitrate metallic containers was evaluated over the last decades [3-8] at the storage temperatures in commercial solar plants (around 390ºC in parabolic trough collectors and 565ºC in central tower receivers) but recently, increased efforts were directed towards understanding the corrosion phenomena at higher temperatures.

The presence of impurities in the molten salt were identified as one of the critical parameters in molten salts corrosion, interfering with the thermal transfer/storage properties including the thermal decomposition of the salts due to the nitrate/nitrite stability at high temperatures (up to 565ºC). Cordaro and Bradshaw [9] studied the thermal stability of the $NaNO_3$:$KNO_3$ system and found that the nitrate/nitrite equilibrium occurs at 220ºC:

$$NO_2^- + \tfrac{1}{2}O_2 \leftrightarrow NO_3^- \quad (1)$$

Considering the equilibrium constant of:

$$K = \frac{[NO_3^-]}{[NO_2^-]} P_{O_2}^{-\frac{1}{2}} \quad (2)$$

This equilibrium constant at 550ºC decreases with increasing temperatures, accelerating the formation of $NO_2^-$ and thus decreasing the thermal stability of the salt. However, at 404ºC, the oxidation rate of $NO_2^-$ to $NO_3^-$ is 10 times faster than the forward reaction. Cordaro and Bradshaw [9] maintained a salt mixture ratio of $[NO_2^-]/[NO_3^-]$:1/1 at 450°C in a conventional furnace, and they observed that after 120 days the nitrate/nitrite ratio increased to 20:1. Observing the behaviour of this ion, the stability must be retained with an inert atmosphere with no oxygen to prevent oxidation of the nitrite anion. The use of an inert atmosphere was studied in the literature [10,11] in order to prevent the nitrite oxidation and extend the thermal stability. Medhi et al. [11] concluded that the use of oxygen blanket gas delays the degradation temperature of the ternary molten nitrate by 55ºC, obtaining a maximum operation temperature of 624ºC in a mixture composed by 13.23wt.% $NaNO_3$ + 57.14wt.% $KNO_3$ + 29.63wt.% $LiNO_3$.

At high temperatures, carbonates are commonly formed by the reaction of nitrates with atmospheric $CO_2$ through the following reactions [12]:

$$2NaNO_3 + CO_2 \leftrightarrow Na_2CO_3 + N_2 + {}^5/_2O_2 \quad (3)$$

$$Na_2O + CO_2 \leftrightarrow Na_2CO_3 \quad (4)$$

Similarly, these formed $CO_3^{2-}$ ions can interact with calcium and/or magnesium impurities to form other carbonate compounds.

Along with these insoluble products, sulphates are also present that can hinder the proper salt fluidity for commercial applications. The available $SO_4^{2-}$ anions can interact with carbonates, as well as with other salt ions, such as calcium and/or magnesium impurities [13-15]:

$$2K^+ + SO_4^{2-} \leftrightarrow K_2SO_4 \quad (5)$$

Zhang et al. [16] analysed the stability of these impurities in $NaNO_3/KNO_3$, finding the formation of MgO and $CO_2$ above 300ºC. They also studied the interaction between $Na_2CO_3$ and $Mg(NO_3)_2{\cdot}6H_2O$ to form $Na_2Mg(CO_3)_2$ through:

$$MgO + Na_2CO_3 + CO_2 \leftrightarrow Na_2Mg(CO_3)_2 \quad (6)$$

Magnesia (MgO) can capture $CO_2$ producing $MgCO_3$, through the following reaction:

$$MgO + CO_2 \leftrightarrow MgCO_3 \quad (7)$$

Above 300ºC, $MgCO_3$ will thermodynamically dissociate to form MgO, which is more stable, and thus, the following reaction can occur:

$$MgO + Na_2CO_3 + CO_2 \leftrightarrow Na_2Mg(CO_3)_2 \quad (8)$$

MgO reacts preferably with $CO_2$ at temperatures up to 520ºC to obtain $Na_2Mg(CO_3)_2$, due to its higher stability. Neither $Na_2CO_3$ nor $MgCO_3$ can form eutectics with $NaNO_3$, although $Na_2CO_3$ is slightly dissolved (3%–4%) in $NaNO_3$ at 400ºC. The molten $NaNO_3$ can penetrate through the grain boundaries of the double salt $Na_2Mg(CO_3)_2$, generating liquids channels that can accelerate the diffusion of $CO_2$.

A recent paper published by Prieto et al. [17] established the influence of magnesium nitrate with the thermal decomposition of solar salt. These authors conclude that $Mg(NO_3)_2$ is the main source of NOx emissions in solar salts during the melting process and the use of vents and abatement systems are needed to avoid the influence of this impurity in the corrosion mechanism.

Moisture in molten salts is one of the most important parameters to consider due to its influence in the corrosion rate. Zambonin et al. [18-21] analysed the influence of water in molten nitrates and its interactions at elevated temperature. They considered the following two stages with different steps:

$$1^{st}\text{ stage:} \quad H_2O + e^- \leftrightarrow OH^- + H \quad (9)$$

$$H + H \leftrightarrow H_2 \quad (10)$$

$$2^{nd}\text{ stage:} \quad H + NO_3^- + e^- \leftrightarrow OH^- + NO_2^- \quad (11)$$

Reaction (11) takes place through the following reactions:

$$H + NO_3^- \leftrightarrow OH + NO_2^- \quad (12)$$

$$OH + e^- \leftrightarrow OH^- \quad (13)$$

Stages (9) and (11) lead to reaction (14), in which two electrons per mole of water are involved:

$$H_2O + NO_3^- + 2e^- \leftrightarrow NO_2^- + 2OH^- \quad (14)$$

In contrast, if the 1st stage is reactions (9) and (10), the reaction is:

$$H_2O + e^- \leftrightarrow OH^- + ½\ H_2 \quad (15)$$

In this step, only one electron per mole of water is required [19, 22].

Zambonin et al. [18] proposed that reaction (15) will be most favoured when the reduction rate of water increases. The study of this phenomenon [20,23] is broadened to determine that hydrogen protons present may form nitric acid by:

$$H^+ + NO_3^- \leftrightarrow HNO_3 \quad (16)$$

Thermal instability of this acid causes rapid decomposition, releasing brown vapours that can be observed during the melting process:

$$2HNO_3 \leftrightarrow 2NO_2 + H_2O + ½\ O_2 \quad (17)$$

Therefore, the excess of water in the salt hinders the formation of peroxide and superoxide ions in the molten nitrate [21].

Peleg [25] studied the solubility of water in molten nitrates and determined a water solubility higher in $NaNO_3$ than in $KNO_3$ at 340°C. The solubility is due to the interaction between the negative side of the water dipole and the positive alkali-metal cation of the salt. The larger charge density in $Na^+$ compared with $K^+$ allows the incorporation of higher water content in $NaNO_3$. From this phenomenon, it can be inferred that the formation of alkali oxides, and their proven inhibitory action in nitrate reduction reaction, has no effect with water-containing salts, because it will slow the formation of oxide, peroxide, or superoxide species and the electronic movement in the molten salt.

Fernandez et al. [26] studied the effect of moisture-reduced environments in the corrosion process of solar salt after lowering its moisture content with thermal treatments before samples immersion. The results showed a significant reduction in corrosion rates from 0.11 to 0.02 μm/h after the salt purification, confirming that water is involved in the corrosion process.

Nitrate molten-salt corrosion mechanism

The corrosive effect of nitrate salts is based on the following reduction reaction:

$$NO_3^- + 2e^- \leftrightarrow NO_2^- + O^{2-} \quad (18)$$

which results in the oxidation of iron from the alloy [26, 27]:

$$Fe + O^{2-} \leftrightarrow FeO + 2e^- \quad (19)$$

$$3FeO + O^{2-} \leftrightarrow Fe_3O_4 + 2e^- \quad (20)$$

To understand this process in alkaline nitrates, it is important to evaluate the formation of several oxidized ions during corrosion. Experiments performed by De Jong et al. [28] indicated the presence of $O^{2-}$ (oxide), $O_2^{2-}$ (peroxide), and $O_2^-$ (superoxide), which arise from unstable oxide ions in the nitrate melt, as described by the following reactions:

$$O^{2-} + NO_3^- \leftrightarrow NO_2^- + O_2^{2-} \quad (21)$$

$$O_2^{2-} + 2NO_3^- \leftrightarrow 2NO_2^- + 2O_2^- \quad (22)$$

Several authors studied the formation of these oxides during corrosion in nitrates [20, 23]. In $Na_2O$ and $KO_2$, $K^+$ and $Na^+$ cations have different affinities for the oxide and superoxide ions formed:

$$2Na^+ + O^{2-} \leftrightarrow Na_2O \quad (23)$$

$$2K^+ + 2O_2^- \leftrightarrow KO_2 \quad (24)$$

The formation of $Na_2O$ and $KO_2$ hinders the electronic transfer required for the cathodic reaction to occur, thus decreasing the corrosive behaviour of the salt.

Furthermore, water may dissociate into $H^+$ and $OH^-$, and $Cl_2$ can be formed by $Cl^-$ reacting with oxygen:

$$2Cl^- + ½O_2 \leftrightarrow Cl_2 + O^{2-} \quad (25)$$

Perchlorates ($ClO_4^-$) are present as impurities in commercial molten nitrates. During the melting process, these impurities need to be reduced as much as possible because at high temperature, perchlorate dissociates into oxygen and chloride:

$$ClO_4^- \leftrightarrow 2O_2 + Cl^- \quad (26)$$

The presence of both oxygen and chlorine exponentially increase the corrosiveness of the salt.

Kleppa et al. [29] determined the influence of steric hindrance between $ClO_4^{2-}$ and $Na^+$ or $K^+$ ions on the formation of compounds, in which $KClO_4$ formation was favoured because the potassium ion is smaller.

## 3. Corrosion Studies Results

Papers found in the literature concerning the corrosion impurity influence caused by molten nitrates with solar TES application focused on solar salt, composed by 60wt.% $NaNO_3$–40wt.% $KNO_3$. Bradshaw et al. [30-32] performed different corrosion tests in austenitic stainless steels and carbon steel (A516) from 400ºC to 565ºC. These studies were conducted with thermal cycling at different salt impurities levels, identifying that chloride levels are directly related to the corrosion ability in these molten salts. This relation is shown in Table 1.

**Table 1. Relation between chloride levels and corrosion rate for A516 immersed in solar salt [30,32].**

| Temperature (°C) | Chloride level (wt.%) | Testing time (hours) | Metal loss ($10^{-3}$ mm) | Annual loss rate (mm/year) |
|---|---|---|---|---|
| 400 | 0 | 810 | 7.2 | 0.078 |
| | 0.5 | 811 | 18.4 | 0.198 |
| | 1.0 | 804 | 37.2 | 0.405 |
| 450 | 0 | 642 | 21.9 | 0.299 |
| | 0.5 | 724 | 60.7 | 0.734 |
| | 1 | 602 | 105.2 | 1.531 |

The corrosion rates measured for carbon steel A516 Grade 70 imply that metal losses during isothermal service at 400°C increase from 0.08 mm/year in a chloride-free molten salt to 0.4 mm/year in 1wt.% chloride. At 450°C, metal losses of 1.5 mm/year in 1wt.% chloride were obtained, whereas in the absence of chloride, the corrosion rate was 0.3 mm/year. The tendency of oxide scale layers to spall depended on the concentration of dissolved chloride. Magnetite was the only corrosion product formed on carbon-steel specimens, regardless of temperature or chloride content. These results allowed the use of this alloy in the first commercial CSP plant with storage (SEGS I). Beyond this development, different authors continued performing corrosion studies applied to CSP plants, proposing new materials for tanks and piping to extend the life time of commercial plants.

Soleimani et al. [33] increased the temperature to 600°C using nitrate solar salt with ferritic steels (P91 and X20CrMoV11), austenitic steels (SS316 and SS347H), and Ni superalloy (IN625) up to 5000 h. The ferritic steels were completely destroyed and dissolution of the oxide corrosion products in the molten salt was observed in the austenitic steels. IN625 exhibited the best protective behaviour among the alloys, showing a linear weight loss with very slow kinetics (Fig. 1). These authors [33] conclude that a multiphase oxide layer composed of iron–chromium spinel, iron oxides, and sodium ferrite was formed on SS347H, and a dense NiO layer was primarily formed on the IN625 surface.

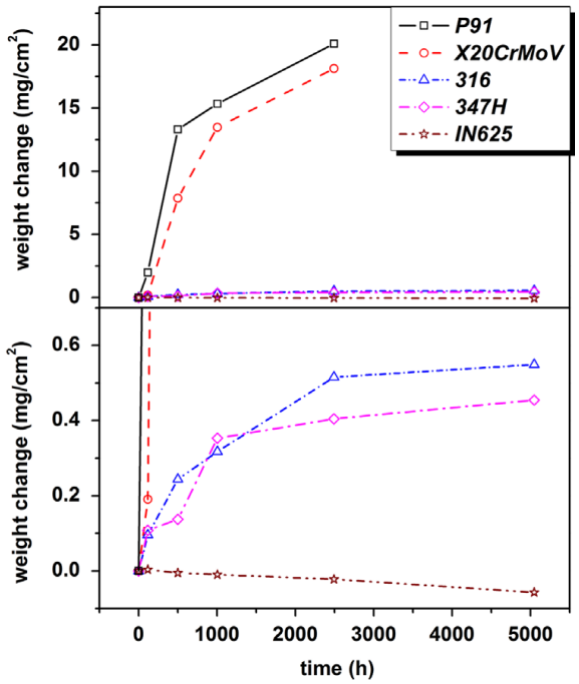


Figure 1. Weight changes of alloys exposed to molten nitrate at 600°C up to 5000 h [33].

Nickel-based materials were proposed as corrosion-resistant materials at temperatures above 600°C. Results for IN624, IN625, and HR230 showed excellent behaviour at temperatures up to 680ºC [34-38] and no impurity influence was detected. On the other hand, when austenitic stainless steels were immersed in molten nitrates at 680ºC, severe spallation was observed (Fig. 2). In this case (Figure 2), it is important to point out the salt line detected in the experiment established a new parameter to take into account for corrosion mechanism elucidation. In this sense, the vapours released during the experiment are also aggressive to the container material. For this reason, Peiro et al. [38] recommend to vent the storage tanks during the molten salt melting process in order to remove the corrosive volatile products.

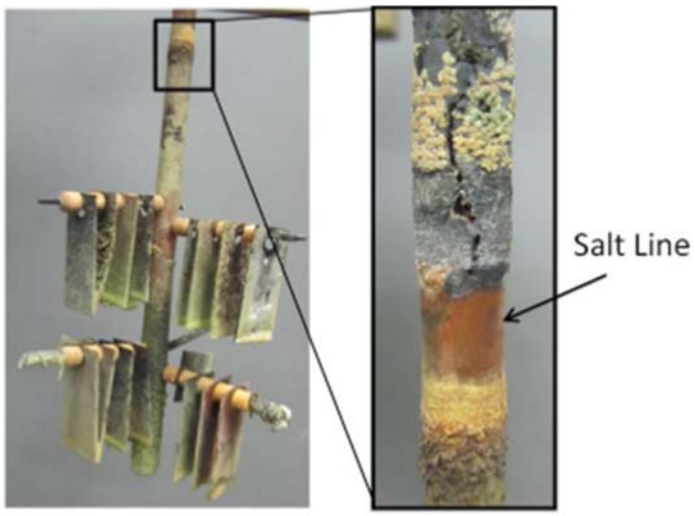


Figure 2. Austenitic steel corrosion at 680°C in contact with nitrate solar salt [34].

Regarding the thermal properties enhancement, nanoparticles were selected to improve the heat transfer performance, nevertheless, these additions can have an influence in the corrosion mechanism. In a recent paper, Fernandez et al. [39] determined that the addition of $Al_2O_3$ nanoparticles (1wt.%) to the solar salt presents an unexpected enhancement in the corrosion resistance for the materials immersed, since nanoparticles formed a protective barrier in the steel surface, changing the corrosion mechanism in this environment. In this direction, Grosu et al. [40] established that the presence of nanoparticles affects the corrosion mechanism in nitrate molten salts, detecting that in nanodoped molten salts ($Al_2O_3/SiO_2$ (1wt.%)) show no influence of the magnesium compounds and a higher corrosion rate, compared to commercial solar salt, was detected in Hitec XL molten salt.

The use of inhibitors and/or coatings to reduce corrosion was evaluated in molten nitrates. Gurr et al. [41] proposed the use of NiVAl coating for P91 steel, obtaining good results in solar salt at 565°C. This steel, with low Cr content, was also used by Soleimani et al. [42] in an aluminizing slurry at 600ºC, obtaining a 5-µm protective layer composed by Na $(Fe,Al)O_2$. This research idea has not been further developed due to the additional costs that would be required in commercial plants to coat the entire system in contact with molten salts.

Fahsing et al. [43] established that for long exposure times (>1000 hours) the chromium content beneath the oxide scale decreases, producing breakaway oxidation. Those authors

also determined that in molten salts with high chloride content, a very thin Fe-Cr oxide protective layer is observed and small amounts of chlorine lead to the preferential formation of chromium chloride instead of ion chloride, so a better behaviour was found due to the Cr enrichment in the steel surface. This phenomenon was also detected by Ruiz-Cabañas et al. [44] evaluating the influence of the chloride concentration in the corrosion mechanism of carbon steel A516. These authors demonstrated the important role of chlorides in the corrosion mechanism, affecting the adherence between oxide layers and the steel tested. Moreover, Kruizenga et al. [34] also demonstrated that impurities tend to drive corrosion and the temperature influence, obtaining dissolution of Cr, Mo and W above 600ºC in nitrate molten salts.

In addition to solar salt, the corrosion mechanism evaluation was extended to ternary alkali and alkaline-earth nitrate mixtures. Different authors studied the corrosion behaviour of Hitec molten salt (40wt.%$NaNO_2$ + 7wt.%$NaNO_3$ + 53wt.%$KNO_3$), obtaining a metallographic corrosion thickness lower than 7 µm in low-Cr alloys at 390°C during 2000 hours of exposure [10, 45]. Other nitrate mixtures were proposed as TES materials, highlighting the use of two additives, $LiNO_3$ and $Ca(NO_3)_2$. Fernandez et al. [46] performed several corrosion tests in carbon steels (A1 and A516) and low-Cr steels (T11 and T22), reporting better behaviour of alloys with increasing Cr content. These new salt mixtures reported a better performance against corrosion compared to binary solar salt. Fernandez et al. [47] conducted corrosion study analysing the insoluble and corrosion products formed (Table 2), yielding lower corrosion rates in the ternary salts containing $Ca(NO_3)_2$, due to a lower $Cl^-$ content.

Table 2. Corrosion products and insoluble salt formed in Hitec XL and solar salt in contact with commercial carbon steels [47].

| **Molten salts** | **Steel** | **Corrosion products** | | **Insoluble salt** | | **Corrosion rate (µm/h)** |
|---|---|---|---|---|---|---|
| | | **Steel** | **Salt** | **Steel** | **Salt** | |
| Solar Salt | A1 | $MgFe_2O_4$, $Fe_2O_3$, MgO | $Fe_2O_3$, $Na_2O$, $MgFe_2O_4$ | $CaCO_3$, $K_2SO_4$ | $CaCO_3$, $Na_2CO_3$ | 0.1108 |

| | | | | | | |
|---|---|---|---|---|---|---|
| | T22 | $Fe_3O_4$, $Fe_2O_3$, FeCr | $Fe_2O_3$, $Na_2O$, $MgFe_2O_4$ | - | $CaCO_3$, $Na_2CO_3$ | 0.0081 |
| Hitec XL Salt | A1 | $Fe_3O_4$, $Fe_2O_3$, $NaFeO_2$ | $KFeO_2$, $NaFeO_2$, $Na_2O$ | $CaCO_3$, $MgCO_3$ | $CaSO_4$, $K_2SO_4$, $(Ca,Mg)CO_3$, $CaCO_3$ | 0.00075 |
| | T22 | $MgCr_2O_4$, $Fe_2O_3$ | $Na_5FeO_4$ | $CaCO_3$, $MgCO_3$ | $CaSO_4$, $CaCO_3$, $(Ca,Mg)CO_3$ | 0.00044 |

In a recent research, Grosu et al. [48] analysed the corrosion mechanism in Hitec XL salt (15wt.%$NaNO_3$ + 43wt.%$KNO_3$ + 42wt.% $Ca(NO_3)_2$), highlighting the formation of two corrosion mechanisms, oxidation (corrosion) and carbonization (protection). Those authors finding allowed the proposal of a simple method to control the corrosion mechanism of carbon steel in contact with nitrate molten salts by spray graphitization. In another paper [58] they also analysed the influence of humidity in the corrosion produced by Hitec XL, obtaining that the corrosion rate for carbon steel increased from 0.011 mm/year to 0.031 mm/year when humidity was introduced into the corrosion reactor. On the other hand, stainless steel 304 was less affected by humidity (0.0070 mm/year versus 0.0076 mm/year).

Cheng et al. [49] focused their research on lithium ternary salts composed by 30wt.% $LiNO_3$–18wt.% $NaNO_3$–52wt.% $KNO_3$ in Cr–Mo steels at 550°C up to 1000 hours proposing a detailed corrosion mechanism (Fig 3). They indicated that during the corrosion process, different Li impurities form $LiFeO_2$ and $LiFe_5O_8$ in the outer scale through the lithiumization of $Fe_2O_3$. It is important to point out that the different oxide scales with Li content present a non-protective scales.

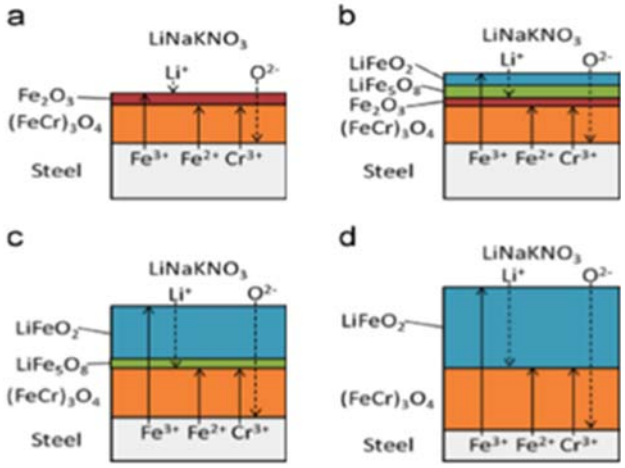


Figure 3. Corrosion layers formed in contact with lithium-containing molten salts at (a) 200 h, (b) 400 h, (c) 600 h, and (d) 800h [49].

Fernandez et al. [50] detected the formation of a 5-µm layer of magnesium-ferrite on the alloy surface due to the presence of Mg-compound impurities in solar salts. These authors also detected the formation of a protective Mg-Cr scale ($MgCr_2O_4$) in alloys containing more than 2wt.% Cr [46,52].

Common impurities present in nitrate molten salts can form other stable corrosion compounds. Saad et al. [51] detected $NaFeO_2$ as the corrosion product in austenitic steels, and Tortorelli [6] identified a protective compound composed of $Na_2CrO_4$. Bradshaw et al. [32] performed a complete study regarding the diffusion of different ions in the corrosion scale formed in SS316 immersed in solar salt during 4084 hours (Fig. 5), identifying sodium as impurity present in the outer layer.

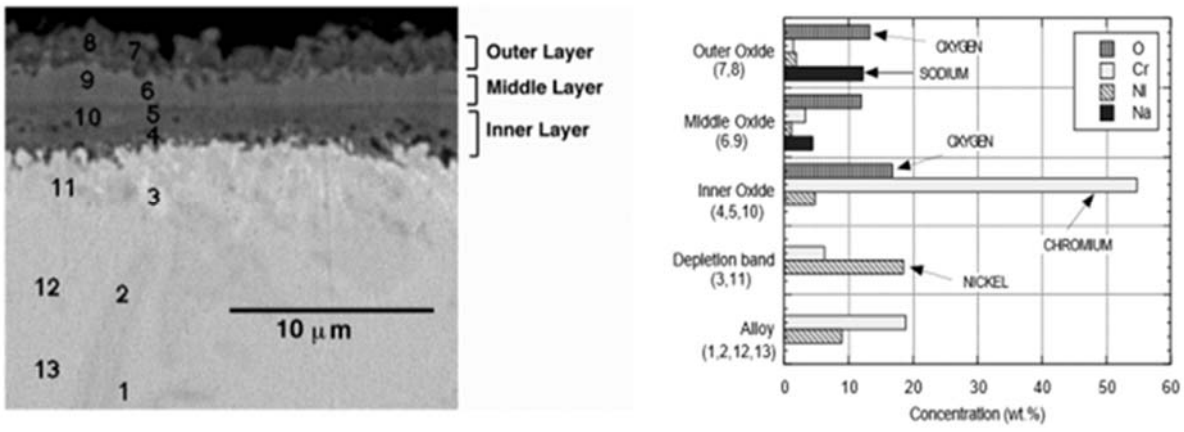

Figure 5. Elemental composition of the corrosion layers produced in SS316 after 4084 h of immersion in solar salt at 565ºC [32].

Some authors analysed the influence of different inert atmospheres (N2, Ar) during the corrosion process [10,11,53]. The presence of inert gas covering the molten salt extends the thermal stability and delays the thermal decomposition which it is directly related with the corrosion process and the formation of oxide impurities [53].

In recent years, some authors evaluated the effect of the dynamic corrosion produced by nitrate molten salts [54,55]. In this case, the corrosion mechanism is accelerated and the corrosion layers are removed from the steel surface due to the molten salt flow rate. A gap regarding the corrosion evaluation under dynamic conditions was detected in order to unify criteria for a proper study. Trying to solve this problem, a new methodology (Dynamic Gravimetric Analysis, DGA) was developed at the University of Barcelona [56]. The amount of oxide formed during thermal treatments can be obtained, avoiding technician handling since the sample is in contact with the cleaning solution defined for each metal in the ASTM G1-03 [57], and it is hung from an analytical balance till the cleaning solution starts to attack the metal after removing all the metal oxide. This point is detected by a slope change in the mass loss vs. time registered obtaining a more accurate corrosion rate results than the ASTM G1-03 standard.

Finally, based on the physical state of the thermal carrier in the solar receiver, CSP stakeholders defined three potential pathways: molten salts, particle, or gaseous [1] for the new generation of CSP plants. The selection of a high-temperature molten-salt chemistry is needed and carbonate as well as chloride salts were selected as the main candidates to be applied [1]. However, the corrosion ability of these salts could be an important problem for their implementation and if nitrate salt could reach their thermal stability until 620ºC an important enhancement of the efficiency in the power block would be obtained**.**

## 4. Conclusions

Corrosion mechanisms in nitrate salts are associated with nitrate reduction reactions. The oxygen-containing anions produced from this reduction process are responsible for the increased corrosion ability of the salt. Chloride ions and moisture are the main important impurities that tend to drive corrosion on nitrate molten salts due to the enhancement of Cr dissolution.

Basicity was found to be an important parameter in the nitrate chemistry to be understood. The activity of oxide ions drives the oxidation process to form passivation layers that act as protective barriers against molten-salt corrosion.

Some statements regarding corrosion mechanism studied can be highlighted:

1. Larger exposure times (>1000h) reduce the chromium content producing breakaway oxidation.
2. Cr, Mo and W are dissolved at temperatures above 600ºC in nitrate molten salts, driving the corrosion process.
3. Salt impurities are involved in the corrosion process, forming non-protective layers ($MgFe_2O_3$, $LiFe_5O_8$, etc.) on the steels. Magnesium impurities interact easily with hematite forming magnesium ferrite ($MgFe_2O_3$) of about 5 μm in thickness. In some cases, a protective $MgCr_2O_4$ layer was detected for steels up to 2% Cr. In ternary salts containing $LiNO_3$ compounds, a lithiumization of $Fe_2O_3$ occurs, producing $LiFeO_2$ or $LiFe_5O_8$.
4. The knowledge acquired in corrosion mitigation for nitrate molten salts can help to understand the corrosion issues associated with higher temperatures. New corrosion inhibitor conditions are under study through carbonization of the samples, producing a very effective barrier to the corrosive impurities in nitrate molten salts.

**Acknowledgements**

The research leading to these results has received funding from Spanish government (ENE2015-64117-C5-1-R (MINECO/FEDER)). The authors would like to thank the Catalan Government for the quality accreditation given to their research group GREiA (2017 SGR 1537). GREiA is a certified agent TECNIO in the category of technology developers from the Government of Catalonia.

## References


1. M. Mehos, C. Turchi., J. Vidal, M. Wagner, Z. Ma, C. Ho, W. Kolb, C. Andraka, A. Kruizenga, Concentrating Solar Power Gen3 Demonstration Roadmap. Technical Report, 2017, NREL/TP-5500-67464.
2. M. Kenisarin, High-temperature phase change materials for thermal energy storage. Renewable and Sustainable Energy Reviews, 2010, 14, Pages 955–970.
3. S. A. Bradford, Corrosion. ASM Handbook, 1987, Metals Park.
4. J. W. Slusser, J.B. Titcomb, M.T. Heffelfinger, and B.R. Dunbobbin, Corrosion in Molten Nitrate-Nitrite Salts. Journal of Metals, 1985, 37, Pages 24–27.
5. R. A. Rapp, Hot corrosion of materials: a fluxing mechanism?. Corrosion Science, 2002, 44, Pages. 209–221.
6. P. F. Tortorelli, J.R. Distefano, Selection of corrosion-resistant materials for use in molten nitrate salts. Oak Ridge National Laboratory Report, 1989.
7. K. Vignarooban, X. Xinhai, A. Arvay, K. Hsu, and A.M. Kanna, Heat transfer fluids for concentrating solar power systems: A review. Applied Energy, 2015, 146, Pages 383–396.
8. K. Federsel, J. Wortmann, and M. Ladenberger, High-temperature and corrosion behavior of nitrate nitrite molten salt mixtures regarding their application in concentrating solar power plants. Energy Procedia, 2015, 69, Pages 618–625.
9. J. G. Cordaro, R.W. Bradshaw, Multicomponent molten salt mixtures based on nitrate/nitrite anions. Solar Energy Engineering, 2011, 133, Pages 1-4.
10. R. Olivares, The thermal stability of molten nitrite/nitrates salt for solar thermal energy storage in different atmospheres. Solar Energy, 2012, 86, Pages 2576-2583
11. M. Medhi, G.A. Brooks, M. Rhamdhani, Thermal analysis of molten ternary lithium-sodium-potassium nitrates. Renewable Energy, 2017, 104, Pages 76-87
12. C. M. Kramer, Z.A. Munir, and J.V. Volponi, Screening tests of sodium nitrate and potassium nitrate decomposition. Solar Energy, 1982, 29, Pages 437–439.
13. O. Abe, T. Utsunomiya, Y. Hoshino, The thermal stability of binary alkali metal nitrates. Thermochimica Acta, 1984, 78, Pages. 251–260.
14. R. W. Bradshaw, D.E. Meeker, High-temperature stability of ternary nitrate molten salts for solar thermal energy systems. Solar Energy Materials, 1990, 21, Pages 51–60.
15. R. Olivares, C. Chen, S. Wright, The Thermal Stability of Molten Lithium–Sodium–Potassium Carbonate and the Influence of Additives on the Melting Point. Journal of Solar Energy Engineering, 2012, 134, Pages 041002-041008

16. K. Zhang, X. Li, Y. Duan, Roles of double salt formation and $NaNO_3$ in $Na_2CO_3$ promoted MgO absorbent for intermediate temperature $CO_2$ removal. International Journal of Greenhouse Gas Control, 2013, 12, Pages 351–358.
17. C. Prieto, F. J. Ruiz-Cabañas, A. Rodríguez-Sanchez, C. Rubio Abujas, A. I. Fernández, M. Martínez, E. Oró, L. F. Cabeza. Effect of the impurity magnesium nitrate in the thermal decomposition of the solar salt. Solar Energy, 2018, In press.
18. E. Desimoni, F. Paniccia, P.G. Zambonin, Solubility and detection (down to 30 p.p.b.) of oxygen in molten alkali nitrates. Journal of Electroanalytical Chemistry and Interfacial Electrochemistry, 1972, 38, Pages 373–379.
19. P. G. Zambonin, V.L. Cardetta, G. Signorile, Solubility and detection of water in the $(Na,K)NO_3$ eutectic melt. Journal of Electroanalytical Chemistry and Interfacial Electrochemistry, 1970, 28, Pages 237–243.
20. P. G. Zambonin, Oxides/oxygen systems in molten alkali nitrates: Remarks and hypotheses concerning recent literature findings. Journal of Electroanalytical Chemistry and Interfacial Electrochemistry, 1973, 45 Pages 451–458.
21. E. Desimoni, F. Palmisano, P.G. Zambonin, Catalytic currents in fused salts: Discharge mechanism of nitrite in molten alkali nitrates. Journal of Electroanalytical Chemistry and Interfacial Electrochemistry, 1977, 84, Pages 315–322.
22. B. Morelli, L. Sabbatini, P.G. Zambonin, Oxygen electrodes in fused salts: Investigation and mechanistic remarks on the system $(Ni)O_2$, $H_2O/OH$ in the (Na, K) $NO_3$ eutectic melt. Journal of Electroanalytical Chemistry and Interfacial Electrochemistry, 1979, 96, Pages 7–17.
23. P. G. Zambonin, On the presence of $NO_2^+$ in molten nitrates. Journal of Electroanalytical Chemistry and Interfacial Electrochemistry, 1971, 32, Pages 1–4
24. F. Palmisano, Catalytic currents in fused salts: Discharge mechanism of nitrite in molten alkali nitrates(II). Journal of Electroanalytical Chemistry and Interfacial Electrochemistry, 1978, 89, Pages 311–320.
25. M. Peleg, Journal of Physical Chemistry, 1967, 71, Pages 868.
26. A. G. Fernandez, H. Galleguillos, F.J. Perez, Thermal influence in corrosion properties of Chilean solar nitrates. Solar Energy, 2014, 109, Pages 125–134.
27. A. Baraka, A. A. El Hosary, Corrosion on Mild Steel in Molten Sodium Nitrate-Potassium Nitrate Eutectic. British corrosion journal, 1976, 11, Pages 44-46.
28. J. M. De Jong, G.H.J. Broers, A reversible oxygen electrode in an equimolar $KNO_3$ $NaNO_3$ melt saturated with sodium peroxide II. A voltammetric study. Electrochimica Acta, 1976, 21, Pages 893–900.

29. O. J. Kleppa, S.V. Meschel, Thermochemistry of anion mixtures in simple fused salt systems. II Solutions of some salts of $MO_4^-$ and $MO_4^{2-}$ anions in the corresponding alkali nitrates. The Journal of Physical Chemistry, 1963, 67, Pages 2750–2753.
30. R. W. Bradshaw, S. Goods, Corrosion of alloys and metals by molten nitrates. Molten Salt Forum, 2003, 7, Pages 117–134.
31. S. H. Goods, R.W. Bradshaw, Corrosion of Stainless Steels and Carbon Steel by Molten Mixtures of Commercial Nitrate Salts. Journal of Materials Engineering and Performance, 2004, 13, Pages 78-87.
32. Bradshaw, R.W., Effect of chloride content of molten nitrate salt on corrosion of A516 carbon steel. Sandia report, 2010.
33. A. Soleimani Dorcheh, R.N. Durham, M.C. Galetz, Corrosion behavior of stainless and low-chromium steels and IN625 in molten nitrate salts at 600 °C. Solar Energy Materials and Solar Cells, 2016, 144, Pages 109–116.
34. Kruizenga, A.M., Gill, D.D., Laford, M., McConohy, G. Corrosion of High Temperature Alloys in Solar Salt at 400, 500 and 680 C. SANDIA National Laboratories report. 2013, Sand 2013-8256.
35. G. McConohy, A. Kruizenga, Molten nitrate salts at 600 and 680 °C: Thermophysical property changes and corrosion of high-temperature nickel alloys. Solar Energy, 2014, 103, Pages 242–252.
36. A. Kruizenga, D. Gill, Corrosion of Iron Stainless Steels in Molten Nitrate Salt. Energy Procedia, 2014, 49, Pages 878–887.
37. S. H. Goods, R.W. Bradshaw, Constant extension rate testing of IN625LCF in molten nitrate salt. Corrosion Science, 1999, 41, Pages 1119–1137.
38. G. Peiró, C. Prieto, J. Gasia, A. Jové, L. F.Cabeza. Two-tank molten salts thermal energy storage system for solar power plants at pilot plant scale: Lessons learnt and recommendations for its design, start-up and operation. Renewable Energy, 2018, 121, Pages 236-248
39. A.G. Fernandez, B. Munoz-Sanchez, J. Nieto-Maestre, A. García-Romero. High temperature corrosion behavior on molten nitrate salt-based nanofluids for CSP plants. Renewable Energy, 2019, 130, Pages 902-909
40. Grosu, Y., Udayashankar, N., Bondarchuk, O., González-Fernández, L. and Faik, A. Unexpected effect of nanoparticles doping on the corrosivity of molten nitrate salt for thermal energy storage. Solar Energy Materials and Solar Cells, 2018, 178, Pages 91-97.
41. M. Gurr, S. Bau, F. Bermeister, M. Wirth, E. Piedra-Gonzalez, K. Krebber, J. Preubner, and W. Pfeiffer, Investigation of the corrosion behavior of NiVAl multilayer coatings in hot salt melts. Surface and Coatings Technology, 2015, 279, Pages 101–111.

42. A. Soleimani Dorcheh, M.C. Galetz, Slurry aluminizing: A solution for molten nitrate salt corrosion in concentrated solar power plants. Solar Energy Materials and Solar Cells. 2016, 146, Pages 8–15.
43. D. Fahsing, C. Oskay, T.M. Meißner, M.C. Galetz. Corrosion testing of diffusion-coated steel in molten salt for concentrated solar power tower systems, Surface and coating technology, 2018, 354, Pages: 46-55
44. F. J. Ruiz-Cabañas, C. Prieto, V. Madina, A. I. Fernández, L. F. Cabeza. Materials selection for thermal energy storage systems in parabolic trough collector solar facilities using high chloride content nitrate salts. Solar Energy Materials and Solar Cells, 2017, 163, Pages 134-147.
45. A. G. Fernandez, M. Cortes, E. Fuentealba, F.J. Perez, Corrosion properties of a ternary nitrate/nitrite molten salt in concentrated solar technology. Renewable Energy. 2015, 80, Pages 177–183.
46. A. G. Fernandez, H. Galleguillos, F.J. Perez, Corrosion Ability of a Novel Heat Transfer Fluid for Energy Storage in CSP Plants. Oxidation of Metals, 2014, 82, Pages 331–345
47. A. G. Fernandez, H. Galleguillos, E. Fuentealba, F.J. Perez, Corrosion of stainless steels and low-Cr steel in molten $Ca(NO_3)_2$ $NaNO_3$ $KNO_3$ eutectic salt for direct energy storage in CSP plants. Solar Energy Materials and Solar Cells. 2015, 141, Pages 7–13.
48. Y Grosu, U Nithiyanantham, A Zaki, A Faik. A simple method for the inhibition of the corrosion of carbon steel by molten nitrate salt for thermal storage in concentrating solar power applications. Materials Degradation, 2018, 2, Number 34.
49. W. Cheng, D. Chen, C. J. Wang, High-temperature corrosion of CrMo steel in molten $LiNO_3$ $NaNO_3$ $KNO_3$ eutectic salt for thermal energy storage. Solar Energy Materials and Solar Cells. 2015, 132, Pages 563–569.
50. A. G. Fernández, M. Lasanta, and F. Pérez, Molten Salt Corrosion of Stainless Steels and Low-Cr Steel in CSP Plants. Oxidation of Metals, 2012, 78, Pages 329–348.
51. O. Saad, Corrosion behaviour of AISI 304 stainless steel in contact with eutectic salt for concentrated solar power plant applications. University of Central Florida, 2013. Master of Science.
52. A. G. Fernandez, F.J. Perez, Improvement of the corrosion properties in ternary molten nitrate salts for direct energy storage in CSP plants. Solar Energy, 2016, 134, Pages 468–478.
53. A. Bonk, M. Braun, A. Hanke, J. Forstner, D. Rückle, S. Kaesche, V. A. Sötz, T. Bauer. Influence of different atmospheres on molten salt chemistry and its effect on steel corrosion. AIP Conference Proceedings, 2018, 2033, Pages 0900031-0900039
54. G. García-Martín, M.I. Lasanta, V. Encinas-Sánchez, M.T. de Miguel, F.J. Pérez, Evaluation of corrosion resistance of A516 Steel in a molten nitrate salt mixture using a

pilot plant facility for application in CSP plants, Solar Energy Materials and Solar Cells, 2017, 161, Pages 226-231.

55. A. G. Fernández, M. Henriquez, A. Mallco, B. Muñoz-Sánchez, J. Nieto-Maestre. Dynamic corrosion tests comparison: Dynamic reactor vs high temperature pilot plant scale setup for Chilean LiNO3 containing molten salt. AIP Conference Proceedings, 2018, 2033, 0900091-0900096.
56. C. Prieto, J. Gallardo, F.J. Ruiz, C. Barreneche, M. Martinez, M. Segarra, A.I. Fernandez. Study of corrosion by dynamic gravimetric analysis (DGA) methodology. influence of chloride content in solar salt. Solar energy materials and solar cells, 2016, 157, Pages 526-532.
57. International ASTM G1-03, Standard practice for preparing, cleaning, and evaluating corrosion test specimens. 2003.
58. Y. Grosu, O. Bondarchuk, A. Faik. The effect of humidity, impurities and initial state on the corrosion of carbon and stainless steels in molten HitecXL salt for CSP application. Solar Energy Materials and Solar Cells, 2018, 174, Pages 34-41.